[3]Edelman, R. and Fortune, O., "A Preliminary Analysis of Mixing and Combustion in Ducted Flows with Application to Ejector Ramjet Technology," General Applied Science Laboratories, Westbury, N.Y., GASL Technical Report No. 658, May 1967.

[4]Siegelman, D. and Fortune, O., "Computer Programs for the Mixing and Combustion of Hydrogen in Air Streams," General Applied Science Laboratories, Westbury, N.Y., GASL Technical Report No. 618, July 1966.

Momentum Transfer to a Surface with a Pulsed Laser

Peter K. Wu* and Peter E. Nebolsine†
Physical Sciences Inc., Woburn, Mass.

Introduction

THE phenomenology of laser material interaction has been of interest for many years and the momentum transfer to a surface by a laser beam has been reported by many investigators.[1-4] This Note will examine the transient momentum transfer in vacuum in the "transparent" limit, where the laser intensity is below the threshold for plasma formation. In vacuum, particulates may come directly from the surface as a result of laser energy deposition and cause vapor breakdown, a complex phenomenon. Schlier, et al.[5] has reported thresholds of order 10^6 W/cm^2 for large 20μ particles for laser pulse width $\sim 10^{-5}$ sec. Here we will consider intensities below this level. Previous studies were concerned primarily with high intensity laser beams.[1-4] In this regime, when solids are irradiated either in vacuum or atmospheric conditions, plasma is formed above the surface and may degrade the efficiency of momentum transfer to the solid.

A. Transient Heat Conduction

A one-dimensional transient heat conduction problem has been formulated for carbon phenolic, and the governing equation can be written as

$$\rho C_p \frac{\partial T}{\partial t} = K\frac{\partial^2 T}{\partial x^2} + (C_p)_g \dot{m}_g \frac{\partial T}{\partial x} + Q_g \dot{W}_g \qquad (1)$$

where ρ is the density of solid; C_p is the specific heat of solid; T is the temperature; t is the time, $(C_p)_g$ is the specific heat of pyrolyzed (resin) gas; $\dot{m}_g$ is the mass flux of pyrolyzed gas; Q_g is the enthalpy of pyrolysis per unit mass of gas generated; $\dot{W}_g$ is the rate of gas generation per unit volume; and x is the axial coordinate. The last two terms represent the energy transfer due to internal gasification (pyrolysis). Equation (1) has been solved by an explicit forward-marching technique in finite difference form with the initial condition $T(x,t=0)=T_0(x)$ and the boundary conditions for $t>0$

$$-K\frac{\partial T}{\partial t} = I_0 - \dot{m}\Delta H - \epsilon\sigma T^4 - \frac{\rho C_p \Delta T}{\Delta t}, \quad x=0$$

$$\frac{\partial T}{\partial x} = 0 \qquad x=L$$

where $\dot{m}$ is the vaporization rate at the surface; ΔH is the heat of vaporization ($=2.6\times 10^4 Kj/Kg$)[6]; ϵ is the emissivity; σ is the Stefan-Boltzmann constant; and I_0 is the laser flux. The pyrolysis reaction rate can be expressed as[6]

$$W_g = A\rho_r^2 \exp\{-(E/RT)\}$$

where A is a constant; ρ_r is the resin density; E is the activation energy of pyrolysis; and R is the gas constant. The resin density is given by

$$\rho_r = \rho_{r_0} - \int_0^t W_g dy$$

and gaseous mass loss due to pyrolysis

$$\dot{m}_g = \int_0^L W_g dy$$

where L is the wall thickness. Finally the recession rate is expressed in an empirical form

$$\dot{m} = \beta_1 \rho(T_s)^{\beta_2} \exp(-\beta_3/T_s)$$

where β's are constants and T_s is the surface temperature. The constants, β's, are function of material properties. For simple ablators, i.e., Teflon, whose decomposition kinetic are known, analytical expressions for β's can be obtained.[7] However, for the complex carbon phenolic ablator, the empirical constants from Ref. 6 will be used.

In formulating this model, we have made several assumptions. Firstly, the laser energy is assumed to be instantaneously absorbed at the surface. This implies that the absorption length in the solid is small compared with the thermal depth for the duration of interest. Secondly, when the phenolic resin decomposes at an elevated temperature which is below the sublimation temperature of carbon, the phenolic gas is assumed to be able to escape through the porous carbon char.

Now Eq. (1) can be solved with the appropriate initial and boundary conditions to provide complete temperature profiles in the solid and the surface recession rates. In the following calculations, the thermodynamic properties of carbon phenolic are taken from Ref. 6. The spectral emissivity of phenolic graphite which has been measured by Chang[8] varies from 0.87 in the visible spectrum to 0.62 in the infrared. However, as shown by Whitson,[9] the emissivity depends also on the type of graphite and its surface conditions. Here the emissivity of carbon phenolic is taken to be 0.81, and the initial temperature, T_0 has been assumed to be 300 K.

B. Coupling Coefficient

The calculation of impulse delivered per unit of incident energy, i.e., the "coupling coefficient," requires some knowledge of the phenomena above the solid surface. When the ambient pressure is either small or nonexisting we can assume that the gas at the surface has a Maxwellian velocity distribution. Then the mass flux per unit area leaving the surface can be readily expressed as a function of vapor pressure and temperature.[10] In the vacuum limit, $T_v = T_s$ and the vapor pressure can be obtained as $p_v = \dot{m}(2\pi R T_s)^{1/2}$. Once the vapor pressure is known, one can now calculate the instantaneous coupling coefficient $C = p_v/I$ and the integrated coupling coefficient

$$C_I = \int_0^t p_v dt \Big/ \int_0^t I dt$$

The definition of C_I is appropriate for comparison with experimental measurements of the net impulse delivered per unit of incident energy. For a sufficiently long laser pulse, the coupling coefficient will rise from zero at the beginning of the

Received Dec. 16, 1976; revision received March 3, 1977.
Index categories: Lasers; Combustion in Heterogeneous Media; Heat Conduction.

*Principal Scientist. Member AIAA.
†Principal Scientist.

pulse and will asymptotically approach the steady-state (constant) value from below. Hence there is no need to continue the calculation once the rate of change of coupling coefficient is smaller than some arbitrarily chosen reference value. Here, the cut-off time, t^*, is defined when

$$\partial \ln C/\partial \ln t = 0.03$$

For intensities of 10^6, 10^5, and 10^4 W/cm^2, one gets $t^* = 4.2\times10^{-4}$, 3×10^{-2}, and 2 sec respectively. We have plotted the coupling coefficients for carbon phenolic as a function of normalized time in Fig. 1. The calculation for a laser intensity of 10^3 W/cm^2 was not completed because t^* was estimated to be 160 sec. The calculations were terminated and the dotted line is an estimate of the steady-state value. The difference between the instantaneous coupling coefficient C and the integrated coupling coefficient C_I is due to the transient enthalpy required to raise the temperature of the material at T_0 to the vaporization temperature. This initial "investment" transient energy becomes a smaller portion of the total energy with increasing time. Hence C_I is observed to asymptotically approach the instantaneous value. As shown in Fig. 1, the steady-state values of the coupling coefficient for carbon phenolic ranges from 12.8 to 15.8 dyne-sec/joule for laser intensity of 10^4 to 10^6 w/cm^2.

C. Short Pulses Effects

In the previous calculations CW operation has been implied. The impulse due to multiple laser pulses of varying duty cycle is also of interest. For simplicity, we will consider only one laser intensity of 10^6 W/cm^2 and illustrate the effects of multiple pulses with four pulses. As shown in Fig. 2, the surface temperature history of four 20 μsec pulses with spacing of 20 μsec has the expected fast rise and slow decay behavior. For the four 20 μsec pulses, the total impulse per unit area, I_p, decreases with increasing spacing, τ_s, Fig. 3, and

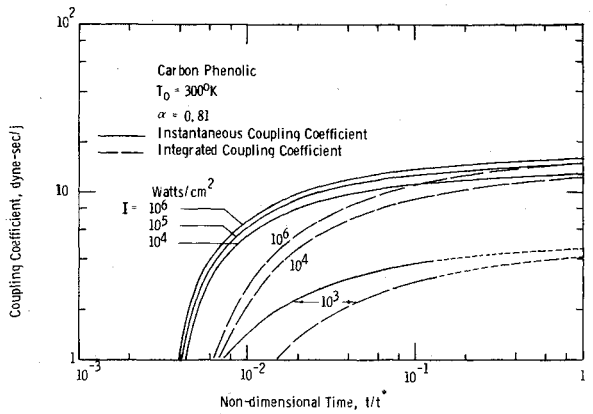

Fig. 1 Time history of coupling coefficient for carbon phenolic.

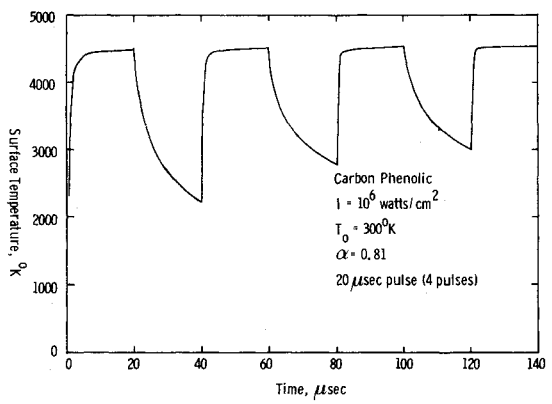

Fig. 2 Surface temperature history for a 4-pulse beam.

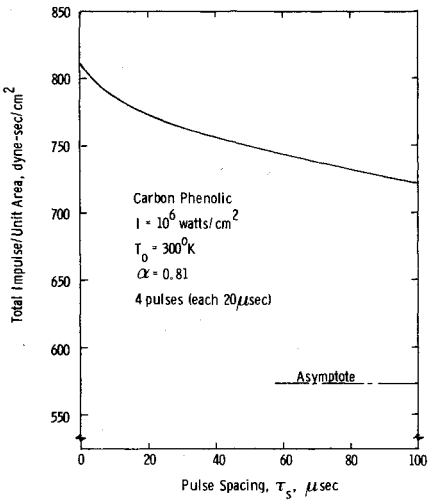

Fig. 3 Total impulse per unit area as a function of pulse spacing.

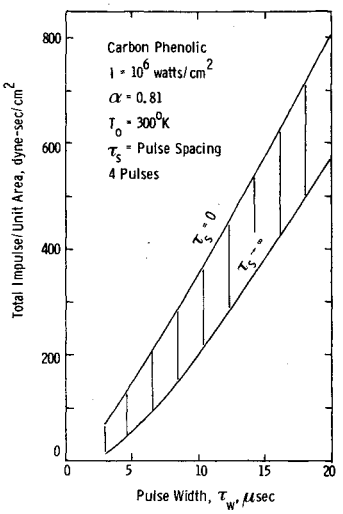

Fig. 4 Total impulse per unit area as a function of pulse width.

it drops from 810 dyne-sec/cm^2 at $\tau_s = 0$ to 722 dyne-sec/cm^2 at $\tau_s = 100$ μsec. The asymptote which is defined as the limiting value as τ_s goes to infinity is 574 dyne-sec/cm^2. Hence, the effects of repetitive pulses are significant at $\tau_s = 100$ μsec. Finally, the effects of pulse width, τ_w, are shown in Fig. 4. The total impulse per unit area, I_p, for four pulses is plotted against the pulse width τ_w. The top curve is the zero spacing value while the bottom curve represents the asymptote for given τ_w. It can be observed that I_p increases with increasing τ_w.

D. Results and Discussion

An interesting comparison may be made between CW and pulsed momentum transfer. Consider a laser beam which delivers four 20 μsec pulses with 100 μsec spacing at an intensity of 10^6 w/cm^2 to a carbon phenolic surface. From Fig. 3, one gets the total impulse per unit area impacted to the surface to be 720 dyne-sec/cm^2. Let's compare this result to that of CW radiation for the same amount of total energy and time. The average intensity over the same time period, i.e., 380 μsec, is about 2.1×10^5 w/cm^2. With this intensity, one gets $t^* = 10^{-2}$ sec, Fig. 2, and hence $t/t^* \simeq 3.8\times10^{-2}$. The corresponding coupling coefficient for $I = 2.1\times10^5$ W/cm^2 and $t/t^* \simeq 3.8\times10^{-2}$, from Fig. 1, is $C \simeq 7.1$. Finally, we can calculate the total impulse per unit area, and it becomes $I_p = CI\tau = 567$ dyne-sec/cm^2. It is interesting to note that in this particular example the total impulse delivered for a given amount of energy is 27% greater in the pulsed mode.

Acknowledgments

This work was sponsored by the Office of Naval Research, under Contract N00014-76-C-0737 and ONR Project Manager, A. D. Wood. The authors express their appreciation to R. Weiss for suggesting this problem, and his helpful comments.

References

[1]Gregg, D. W. and Thomas, S. J., "Momentum Transfer Produced by Focused Laser Giant Pulses," *Journal of Appplied Physics*, Vol. 37, June 1966, pp. 2787-2789.

[2]Skeen, C. H. and York, C. M., "Laser-Induced 'Blow-Off' Phenomena," *Applied Physics Letters*, Vol. 12, June 1968, pp. 369-371.

[3]Pirri, A. N., Schlier, R. and Northam, D., "Momentum Transfer and Plasma Formation Above a Surface with a High-Power CO_2 Laser," *Applied Physics Letters*, Vol. 21, Aug. 1972, pp. 79-81.

[4]Pirri, A. N., "Theory for Momentum Transfer to a Surface with a High-Power Laser," *The Physics of Fluids*, Vol. 16, Sept. 1973, pp. 1435-1440.

[5]Schlier, R. E., Pirri, A. N., Reilly, D. J., "Air Breakdown Studies," Air Force Weapons Lab., Kirtland Air Force Base, N. Mex., AFWL-TR-72-74, 1972.

[6]Weber, G. A. and Bartle, R. R., "Thermal Design Properties Handbook," Avco/MSD, Wilmington, Md., KHDR-AVMSD-68-3, May 1968.

[7]Kemp, N. H., "Surface Recession Rate of an Ablating Polymer," *AIAA Journal*, Vol. 6, Sept. 1968, pp. 1790-1791.

[8]Chang, J. and Sutton, G. W., "Spectral Emissivity Measurements of Ablating Phenolic Graphite," *AIAA Journal*, Vol. 7, June 1969, pp. 1110-1114.

[9]Whitson, Jr., M. E., "Handbook of the Infrared Optical Properties of Al_2O_3, Carbon, MgO, and ZrO_2," The Aerospace Corporation, El Segundo, Calif., SAMSO-TR-75-131, Vol. I, June 1975.

[10]Kennard, E. H., *Kinetic Theory of Gases*, McGraw-Hill, New York, 1938.

Base Pressure on Sharp and Blunt Conical Bodies at Supersonic Speeds

R. F. Starr*
Arnold Engineering Development Center, Arnold Air Force Station, Tenn.

Nomenclature

B = nose bluntness ratio, d_n/d_B
d_B = cone base diameter
d_n = cone nose diameter
M_B = blunt cone surface Mach number just ahead of the base, inviscid
M_{eff} = effective Mach number of flow into base region, Eq. (1)
M_S = sharp cone surface Mach number, inviscid
M_∞ = freestream Mach number
M'_{eff} = effective Mach number, M_{eff}, isentropically expanded through cone semiangle (back to parallel)
P_B = cone base pressure
P_c = cone surface pressure just ahead of the base
P_∞ = freestream pressure
P'_c = cone surface pressure, P_c, isentropically expanded through cone semiangle (back to parallel)
θ_c = cone semiangle, deg

Received Sept. 7, 1976; revision received March 7, 1977.
Index category: Supersonic and Hypersonic Flow.

*Engineer, 4T Projects Branch, Propulsion Wind Tunnel Facility. Member AIAA.

Introduction

THE base drag of a conical body in supersonic flight represents a large fraction of the total vehicle drag. Twenty to sixty percent of the total drag can be associated with the base flow dependent on cone geometry, Mach number, and Reynolds number. Since the base drag fraction is so large and the difference between the base and freestream pressures can be small, a very precise assessment of base pressure is required if an accurate measurement of total drag is sought. With regard to wind tunnel testing, the test Reynolds number, sting geometry, and bow shock wave reflection from the tunnel wall must be carefully controlled to obtain the required accuracy.

A recent study at AEDC has produced a simple, but very accurate, correlation of the cone base pressure in fully turbulent flow at Mach numbers of 1.5 to 8. The fully turbulent base pressure data used in the correlation have been obtained in the supersonic tunnels at AEDC over the past two decades. The correlation is presented to permit an accurate prediction of supersonic base drag which can then be coupled with an analytically or experimentally determined forebody drag to predict total drag.

Correlation

Several early investigators[1-3] detected that the base pressure on various bodies could be correlated by using the local flow condition just ahead of the base as the nondimensionalizing term. Whitfield and Potter[3] found that the base pressure in a sharp cone flowfield yielded an acceptable correlation curve by using the local cone static pressure, p_c, and local cone Mach number isentropically expanded through the cone semiangle (back to parallel flow). In addition, the effect of bluntness on the base pressure could be accounted for if an "effective" local Mach number were used in the correlation. Comparing sharp nose to 0.3 bluntness cone data, a simple average of the sharp cone surface Mach number and blunt cone surface Mach number for any given cone angle and freestream Mach number appeared to be a suitable "effective" Mach number for the blunt body flow. With more extensive data since the work of Ref. 3, an improved form of an effective Mach number for blunt conical bodies has been established. This effective Mach number takes the form

$$M_{\text{eff}} = M_S - (M_\infty/3)B(M_S - M_B) \qquad (1)$$

In this expression, the bluntness ratio, B, and freestream Mach number are seen to weight the effective Mach number closer to the sharp cone surface value, M_S, or the blunt cone surface value, M_B, than a simple average. Physically, the expression may be explained with the aid of Fig. 1. Outside of the entropy layer, the sharp cone and blunt cone flow Mach numbers are identical for a given freestream condition and cone angle. Inside the entropy layer, the Mach numbers digress. The relative thickness of the entropy layer is dependent on the bluntness ratio and the thickness of the fluid layer influencing the wake. Hence, the inviscid surface Mach number M_B is not, in itself, representative of the properties of the total fluid layer which influence the wake for a blunt body and must be weighted with the other region flow. However, it can be shown that the variation in static pressure through this layer is small, such that the cone (either sharp or blunt) surface pressure is an adequate parameter. The inviscid cone surface properties used in Eq. (1) are obtained from existing computer flowfield solutions or table lookup.

This semiempirical technique has been found to correlate an extensive collection of AEDC/VKF turbulent base pressure data between Mach 2 and 8 for cone semiangles from 6 to 14 deg and bluntness ratios from sharp up to 0.7. In essence, the base pressure achieved on a conical body for fully turbulent flow is directly related to a weighted Mach number and the local surface pressure in the layer of fluid just ahead of the base when expanded back to the parallel. Base pressure